Ren et al. Nanoscale Research Letters (2015) 10:60
DOI 10.1186/s11671-014-0713-2

Nanoscale Research Letters
a SpringerOpen Journal

NANO EXPRESS Open Access

Catalytic activities of noble metal atoms on WO_3 (001): nitric oxide adsorption

Xiaoyan Ren[1,3], Shuai Zhang[1], Chong Li[1,2], Shunfang Li[1,2], Yu Jia[1,2*] and Jun-Hyung Cho[4*]

Abstract

Using first-principles density functional theory calculations within the generalized gradient approximation, we investigate the adsorption of NO molecule on a clean WO_3(001) surface as well as on the noble metal atom (Cu, Ag, and Au)-deposited WO_3(001) surfaces. We find that on a clean WO_3 (001) surface, the NO molecule binds to the W atom with an adsorption energy (E_{ads}) of −0.48 eV. On the Cu- and Ag-deposited WO_3(001) surface where such noble metal atoms prefer to adsorb on the hollow site, the NO molecule also binds to the W atom with $E_{ads} = -1.69$ and −1.41 eV, respectively. This relatively stronger bonding of NO to the W atom is found to be associated with the larger charge transfer of 0.43 *e* (Cu) and 0.33 *e* (Ag) from the surface to adsorbed NO. However, unlike the cases of Cu-WO_3(001) and Ag-WO_3(001), Au atoms prefer to adsorb on the top of W atom. On such an Au-WO_3 (001) complex, the NO molecule is found to form a bond to the Au atom with $E_{ads} = -1.32$ eV. Because of a large electronegativity of Au atom, the adsorbed NO molecule captures the less electrons (0.04 *e*) from the surface compared to the Cu and Ag catalysts. Our findings not only provide useful information about the NO adsorption on a clean WO_3(001) surface as well as on the noble metal atoms deposited WO_3(001) surfaces but also shed light on a higher sensitive WO_3 sensor for NO detection employing noble metal catalysts.

Keywords: Surface; Catalytic; Charge transfer; Bond length

Background

NO*x* gases such as NO and NO_2 which are produced from the reaction of nitrogen and oxygen gases in the air during combustion damage not only our environment including air pollution and land contamination but also human health. Therefore, it has attracted much attention in recent years to develop a high-performance NO*x*-sensing equipment [1-4]. For the detection of NO*x*, a number of gas sensors using semiconducting metal oxides such as ZnO [5-7], MoO_3 [8,9], In_2O_3 [10], SnO_2 [11,12], TiO_2 [13], and WO_3 [14] have been reported theoretically and experimentally.

Tungsten oxide (WO_3) has many unusual properties which make it suitable for various applications, e.g., high sensitivity of reducing and oxidizing gases [14], excellent electron transport and photosensitivity, and high stability-resisting photocorrosion in aqueous solvent [15-20]. Especially, WO_3 sensors have been widely applied for the detection of NO*x* gases [21-23]. In order to enhance the performance for NO_2 detection, WO_3 sensors have utilized the addition of metal atoms [24,25] as catalysts. However, there have been relatively few reports for the WO_3 sensor detecting NO molecule [26,27], and furthermore, theoretical studies for the adsorption of NO on WO_3 surfaces are still lacking. In this sense, an accurate first-principles density functional theory (DFT) calculation for the NO adsorption on WO_3 surfaces is highly desirable for the application of WO_3 sensors to NO detection.

In this work, we perform a first-principles DFT calculation to investigate the adsorption of NO molecule on a clean WO_3(001) surface as well as on the noble metal atom (Cu, Ag, and Au) deposited WO_3(001) surface. Here, the (001) surface (see Figure 1a,b) of γ-monoclinic WO_3 is taken into account because it is the most stable at room temperature [28]. We demonstrate that the Cu-, Ag-, and Au-deposited WO_3(001) surfaces exhibit different catalytic behaviors for NO adsorption, that is, the magnitude of adsorption energy (E_{ads}) is in the order of

* Correspondence: jiayu@zzu.edu.cn; chojh@hanyang.ac.kr
[1]International Laboratory for Quantum Functional Materials of Henan, and School of Physics and Engineering, Zhengzhou University, Zhengzhou 450001, China
[4]Department of Physics and Research Institute for Natural Sciences, Hanyang University, 17 Haengdang-Dong, Seongdong-Ku, Seoul 133-791, Korea
Full list of author information is available at the end of the article

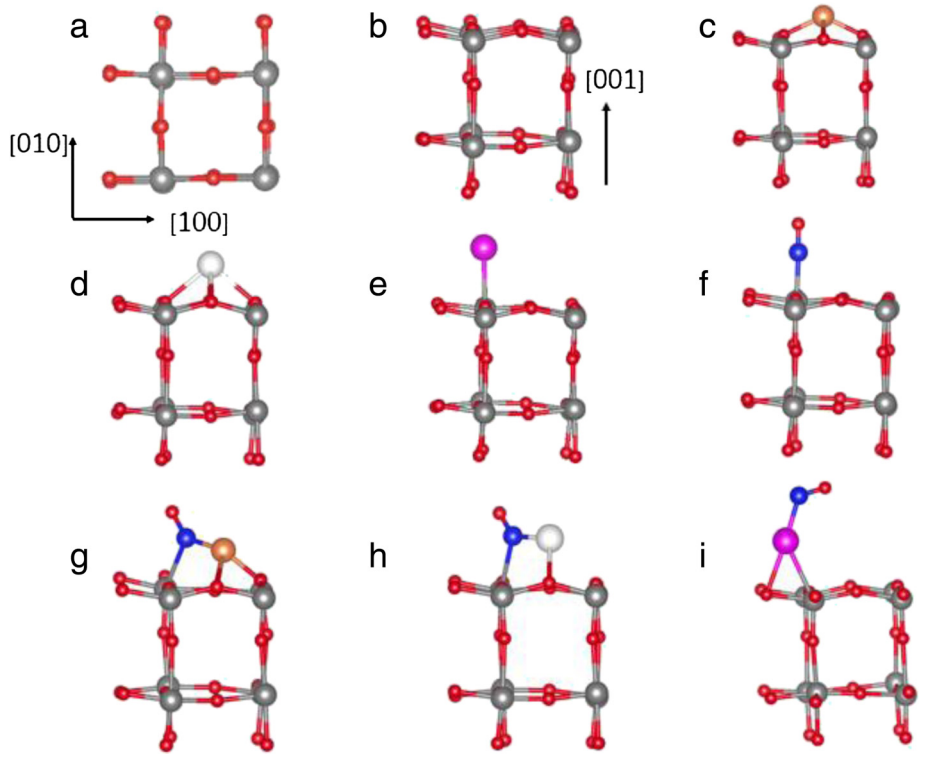

Figure 1 Optimized atomic structure. (a) Top view and **(b)** side view of the clean WO_3 (001) surface. The large and small circles represent W and O atoms, respectively. The most stable structures for the Cu, Ag, and Au atoms deposited on WO_3 (001) surface are displayed in **(c)**, **(d)**, and **(e)**, respectively. The most stable structures for NO adsorption on a clean WO_3 (001) surface and the Cu-, Ag-, and Au-deposited WO_3 (001) surfaces are displayed in **(f)**, **(g)**, **(h)**, and **(i)**, respectively. In **(f)**, **(g)**, **(h)**, and **(i)**, the circle for N atom is larger than that for the O atom.

Cu > Ag > Au. This different binding behavior of NO on WO_3(001) depending on the noble metal species can be traced to the difference in charge transfer from the substrate to adsorbed NO molecule. Based on our DFT results, we will discuss the enhanced sensitivity of WO_3 sensors for NO detection by employing the noble metal catalysts.

Methods

Our DFT calculations were performed using Vienna *ab initio* simulation package (VASP) with the projector augmented wave method [29-32]. For the exchange-correlation energy, we employed the generalized gradient approximation functional of Perdew-Burke-Ernzerhof [33]. The electronic wave functions were expanded in a plane wave basis with an energy cutoff of 400 eV. The WO_3(001) surface was modeled by a periodic four-atomic-layer slab composing two alternate WO_2 plus O layers with approximately 16 Å of vacuum in between the slabs. The *k*-space integration was carried out using a Monhkorst-Pack grid [34] of $4 \times 4 \times 1$ *k* points in the surface Brillouin zone of the monoclinic (1×1) unit cell whose size is as large as the cubic (2×2) unit cell. We relaxed all atoms except the bottom layer along the calculated forces until all the residual force components were less than 0.01 eV/Å. For the interaction of the NO molecule with the clean and metal-deposited WO_3(001) surfaces, we initially placed the NO molecule about 3.5 Å away from the surfaces and obtained the adsorption structure by fully structural optimization.

Results and discussion

NO adsorption on a clean WO_3 (001) surface

We first investigate the adsorption of a single NO molecule on a clean WO_3 (001) surface. Figure 1a,b shows the top and side views of the optimized WO_3 (001) surface, respectively. For the adsorption of NO on WO_3 (001), we consider the three different adsorption sites such as top W (hereafter denoted as S_1), top O (S_2), and hollow (S_3) sites. We find that the N atom of NO is bonding to the substrate atoms, consistent with a previous theoretical calculation [21]. However, in the hollow site, the O atom of NO can be bound to the substrate atoms (denoted as S_4). We calculate the adsorption energy defined as [35] $E_{ads} = E(\text{NO/surf}) - E(\text{surf}) - E(\text{NO})$, where E(NO/surf) is the total energy of the NO-adsorbed WO_3 (001) system, E(surf) is the energy of a clean WO_3 (001) before NO adsorption, and E(NO) is the energy of a free NO molecule, obtained using a $12 \times 12 \times 12$ Å^3 supercell calculation. As shown in Figure 1f, the S_1 configuration is

found to be the most stable with $E_{ads} = -0.48$ eV, larger in magnitude than $E_{ads} = -0.05$, −0.05, and −0.03 eV for S_2, S_3, and S_4, respectively; see Figure 2a. We note that, in the S_1 configuration, the bond length $d_{N\text{-}W}$ between the N and W atoms is calculated to be 2.07 Å, which is much shorter than the sum (3.7 Å) of van der Waals radius of the two atoms [14,36]. Thus, we can say that NO molecule can form a chemical bond with the WO_3 (001) surface.

To evaluate charge transfer in the S_1 configuration, we perform Bader charge analysis for NO before and after its adsorption on the WO_3(001) surface [37,38]. The results for a free NO molecule and adsorbed NO on various substrates are given in Table 1. We find that, upon NO adsorption on a clean WO_3(001) surface, the electrons in the N (O) atom increase (decrease) from 4.44 (6.56) to 4.84 (6.35) *e*, giving rise to an increase of 0.19 *e* in adsorbed NO molecule. This fact shows that adsorbed NO molecule captures electrons from the WO_3(001) surface, indicating that NO behaves as a charge accepter. Indeed, the charge density difference, defined as $\Delta\rho = \rho_{NO/WO3} - (\rho_{NO} + \rho_{WO3})$, clearly shows a charge transfer from the O (in NO molecule) and W atoms to the N atom; see Figure 3a. As a consequence of the additional electrons in NO in the NO/WO_3(001) system, the bond length $d_{N\text{-}O}$ of NO molecule slightly increases to 1.181 Å, compared to that (1.170 Å) of a free NO molecule; see Table 1.

It is noteworthy that the abovementioned charge transfer from the WO_3(001) surface to NO molecule leads to a reduction of conduction electrons in WO_3 (001), thereby forming the electron-depleted layer at the surface. This change of electrical character at the WO_3 (001) surface can be utilized to the WO_3 gas sensor where the contact resistance can be affected by the exposure of NO gas.

Table 1 Charge analysis and bond length of NO molecule

	NO	NO/WO_3	NO/Cu-WO_3	NO/Ag-WO_3	NO/Au-WO_3
N (e)	4.44	4.84	5.00	4.91	4.64
O (e)	6.56	6.35	6.43	6.42	6.40
N + O (e)	11	11.19	11.43	11.33	11.04
$d_{N\text{-}O}$ (Å)	1.170	1.181	1.212	1.203	1.182

Bader charges of N and O atoms in a clean WO_3(001) surface and various noble metal atom-deposited WO_3(001) surfaces are given. Bader charges of N and O atoms in an isolated NO molecule are also given in the first column. The bond length $d_{N\text{-}O}$ in each system is also given.

NO adsorption on Cu- or Ag-deposited WO_3 (001) surface

We begin to optimize the adsorption structure of Cu or Ag on WO_3(001). We find that the adsorption of Cu (Ag) on the hollow site is more stable than the other adsorption sites such as top W and top O sites by 0.66 (0.14) and 0.75 (0.14) eV, respectively. Using Bader charge analysis, we find that the adsorption of Cu and Ag on the hollow site loses electrons to the WO_3(001) substrate by 0.7 and 0.6 *e*, respectively. Using the most stable adsorption configuration of Cu or Ag on WO_3(001), we continue to study the adsorption of NO on such noble metal atom-deposited WO_3(001) substrates. We consider three different adsorption configurations of NO, where N atom is

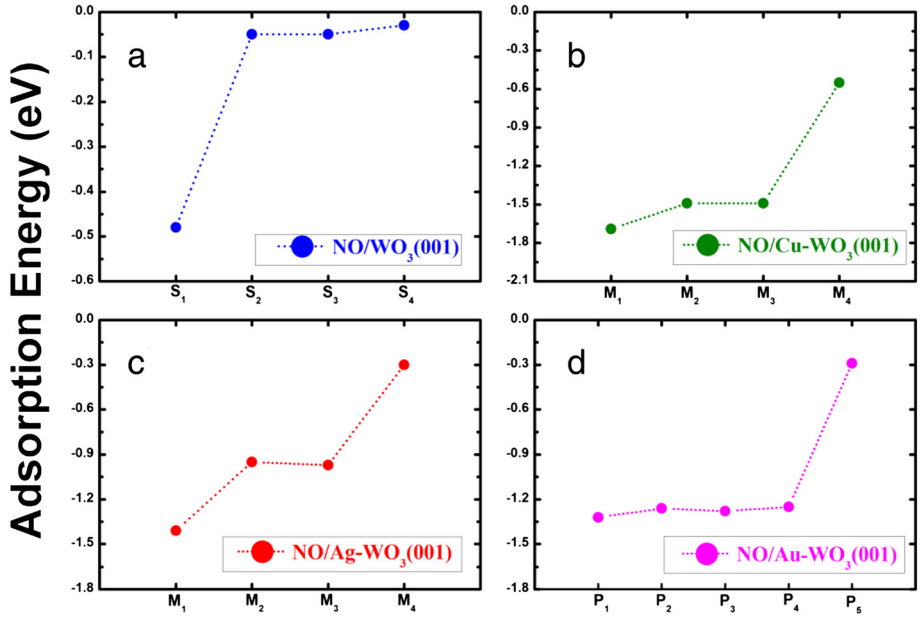

Figure 2 Adsorption energies of various configurations calculated for NO adsorption. NO molecule adsorbed on the **(a)** clean, **(b)** Cu-deposited, **(c)** Ag-deposited, and **(d)** Au-deposited WO3 (001) surfaces. The adsorption configurations such as [S_1, S_2, S_3, S_4], [M_1, M_2, M_3, M_4], and [P_1, P_2, P_3, P_4, P_5] are described in the text.

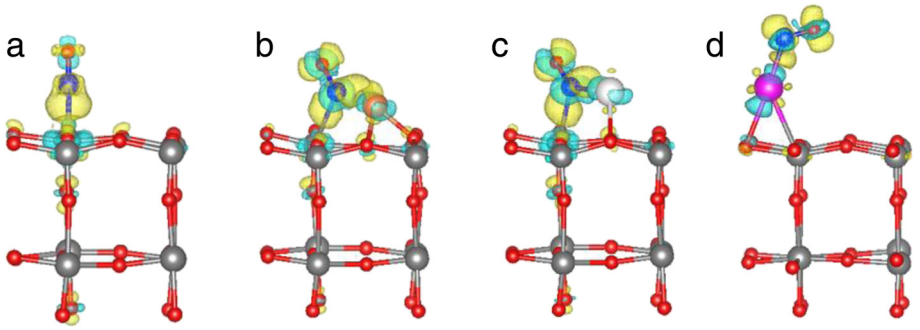

Figure 3 Charge density difference for the most stable configurations of NO adsorption. NO molecule adsorbed on the **(a)** clean, **(b)** Cu-deposited, **(c)** Ag-deposited, and **(d)** Au-deposited WO_3 (001) surfaces. The gain and loss of electrons are drawn in bright and dark colors with an isosurface of 0.005 e/Å^3, respectively.

attached to W (denoted as M_1), O (M_2), and Cu or Ag (M_3) atoms. In addition, we also consider another adsorption configuration of NO, where O atom in NO molecule is attached to Cu or Ag atom (denoted as M_4). The calculated adsorption energy of NO for each adsorption configuration on Cu-WO_3(001) and Ag-WO_3 (001) is given in Figure 2b,c, respectively. We find that the M_1 configuration is the most stable with $E_{ads} = -1.69$ and −1.41 eV for NO/Cu-WO_3(001) and NO/Ag-WO_3 (001), respectively, which are much larger in magnitude than $E_{ads} = -0.48$ eV of the S_1 configuration at a clean WO_3(001) surface. This indicates that Cu and Ag increases the strength of NO binding on WO_3(001), thereby serving as catalysts. In the M_1 configuration, the N atom is also bonding to the W atom with $d_{N\text{-}Cu/Ag}$ (bond length between N and Cu or Ag atoms) = 1.86 or 2.19 Å because of a Coulomb interaction between the negatively charged N atom and the positively charged Cu or Ag atom (see Figure 3b,c), as discussed below. We note that the values of $d_{N\text{-}W}$ amount to 2.36 and 2.37 Å for NO/Cu-WO_3(001) and NO/Ag-WO_3(001), respectively. These values become longer than $d_{N\text{-}W} = 2.07$ Å in the S_1 configuration but are still much shorter than the sum (3.7 Å) of van der Waals radius of N and W atoms [14,36], therefore concluding that NO molecule adsorbs chemically on the Cu-WO_3 (001) and Ag-WO_3(001) substrates.

In Table 1, we find that for the M_1 configuration of NO/Cu-WO_3(001), the electrons in the N (O) atom increase (decrease) from 4.44 (6.56) to 5.00 (6.43) *e*, giving rise to an increase of 0.43 *e* in adsorbed NO molecule. On the other hand, for the M_1 configuration of NO/Ag-WO_3(001), the electrons in the N (O) atom are found to increase (decrease) from 4.44 (6.56) to 4.91 (6.42) *e*, giving rise to an increase of 0.33 *e* in adsorbed NO molecule. These results indicate that adsorbed NO molecule on Cu-WO_3(001) and Ag-WO_3(001) captures more electrons from the substrates compared to the case of NO adsorption at a clean WO_3(001) surface, where only 0.19 *e* is transferred from WO_3(001) to NO. As shown in Figure 3b,c, the calculated charge density difference $\Delta\rho$ shows charge transfer from the O (in NO molecule) and Cu-WO3(001) or Ag-WO3(001) substrate to the N atom, leading to the polar NO molecule with a negatively charged N atom. We note that, as a consequence of the presence of excess electrons in the polar NO molecule, the bond length $d_{N\text{-}O}$ of NO molecule increases to 1.212 and 1.203 Å for NO/Cu-WO_3(001) and NO/Ag-WO_3(001), respectively. These values of $d_{N\text{-}O}$ are longer than $d_{N\text{-}O} = 1.181$ Å for NO/WO_3(001) as well as $d_{N\text{-}O} = 1.170$ Å of a free NO molecule.

Since more electrons transfer from the substrate to adsorbed NO molecule by the deposition of Cu or Ag atoms, one expects an enhanced reduction of conduction electrons in WO_3(001), therefore increasing the sensitivity of WO_3 sensor for NO detection. As a matter of fact, a recent experimental study showed that the deposition of Ag atoms in WO_3 sensor improves its sensitivity for NO detection [27]. We note that, even though NO adsorption induces more electron transfer from the Cu-WO_3(001) substrate compared to Ag-WO_3(001), Cu atoms would be easily oxidized at a usual operation temperature (above 150°C) of WO_3 sensor. This oxidizing effect in noble metal atoms should be cautioned for the gas-sensing performance of WO_3 sensor.

NO adsorption on Au-deposited WO_3 (001) surface

We first optimize the adsorption structure of Au on WO_3(001). Unlike the cases of Cu and Au catalysts, Au atom adsorbs only on top of the W atom, as shown in Figure 1e. Here, the adsorption of Au captures electrons from the WO_3(001) substrate by 0.34 *e* because of a high electronegativity of Au atom. For the adsorption of NO on Au-WO_3(001), we consider several adsorption configurations of NO, where N atom is attached to Au (denoted as P_1), top W (P_2), top O (P_3), and hollow (P_4) sites. In addition, we also consider another adsorption configuration of NO, where O atom in NO molecule is attached to Au atom (P_5). The calculated adsorption energy of

NO for each adsorption configuration on Au-WO_3(001) is displayed in Figure 2d. We find that the P_1 configuration is the most stable with $E_{ads} = -1.32$ eV, which is relatively smaller in magnitude than $E_{ads} = -1.69$ and −1.41 eV for the M_1 configurations of NO/Cu-WO_3(001) and NO/Ag-WO_3(001), respectively. In the P_1 configuration, the calculated bond length of adsorbed NO is $d_{N\text{-}O} = 1.182$ Å (see Table 1), which is shorter than 1.212 and 1.203 Å for NO/Cu-WO_3(001) and NO/Ag-WO_3(001), respectively. This shortest value of $d_{N\text{-}O}$ is due to the fact that NO captures the least electrons (0.04 *e*) from Au-WO_3(001), as shown in Table 1. These features of NO/Au-WO_3(001) such as the smaller adsorption energy, the shorter bond length, and the less electron capture of adsorbed NO is traced to a large electronegativity of Au.

Conclusions

We have performed first-principles DFT calculations within the generalized gradient approximation for the adsorption of NO molecule on a clean WO_3(001) surface as well as on the Cu-deposited, Ag-deposited, and Au-deposited WO_3 (001) surfaces. We found that the NO molecule prefers to adsorb on the top of W atom at a clean WO_3(001) surface, where a charge transfer from WO_3(001) to NO occurs by 0.19 *e* and E_{ads} is calculated to be −0.48 eV. We also found that, on the Cu- and Ag-deposited WO_3(001) surface, the NO molecule also binds to the W atom with $E_{ads} = -1.69$ and −1.41 eV, respectively, accompanying the relatively larger charge transfer of 0.43 *e* (Cu) and 0.33 *e* (Ag) to adsorbed NO compared to the clean WO_3(001) surface. On the other hand, Au atoms on WO_3(001) prefer to adsorb on the top of W atom, and the NO molecule forms a bond to the Au atom with a small electron transfer of 0.04 *e* to adsorbed NO. We obtained a relatively smaller adsorption energy of $E_{ads} = -1.32$ eV for the NO/Au-WO_3 (001) system compared to NO/Cu-WO_3(001) and NO/Ag-WO_3(001) because of a large electronegativity of Au atom. The present results demonstrated that the sensitivity of WO_3 sensors for NO detection can be improved by employing the noble metal catalysts such as Cu and Ag atoms.

Competing interests

The authors declare that they have no competing interests.

Authors' contributions

XYR, YJ, and JHC conceived the central ideas and drafted the manuscript. XYR carried out the calculations. SZ, CL, and SFL participated in the design of the study and discussed the result. All authors read and approved the final manuscript.

Author details

[1]International Laboratory for Quantum Functional Materials of Henan, and School of Physics and Engineering, Zhengzhou University, Zhengzhou 450001, China. [2]Center for Clean Energy and Quantum Structures, Zhengzhou University, Zhengzhou 45001, China. [3]School of Mechanical and Electrical Engineering, Henan Institute of Science and Technology, Xinxiang 453003, China. [4]Department of Physics and Research Institute for Natural Sciences, Hanyang University, 17 Haengdang-Dong, Seongdong-Ku, Seoul 133-791, Korea.

Received: 18 October 2014 Accepted: 23 December 2014
Published online: 11 February 2015

References

1. Huang L, Wang Z, Zhang J, Pu J, Lin Y, Xu S, et al. Fully printed, rapid-response sensors based on chemically modified graphene for detecting NO_2 at room temperature. ACS Appl Mater Inter. 2014;6:7426–33.
2. Fowler JD, Allen MJ, Tung VC, Yang Y, Kaner RB, Weiller BH. Practical chemical sensors from chemically derived graphene. ACS Nano. 2009;3:301–6.
3. Rout CS, Ganesh K, Govindaraj A, Rao CNR. Sensors for the nitrogen oxides, NO_2, NO and N_2O, based on In_2O_3 and WO_3 nanowires. Appl Phy A-Mater. 2006;85:241–6.
4. Ratnawati L, Morton J, Henry RL, Thomas PS. Exhaled breath condensate nitrite/nitrate and pH in relation to pediatric asthma control and exhaled nitric oxide. Pediatric Pulm. 2006;41:929–36.
5. Breedon M, Spencer MJS, Yarovsky I. Adsorption of NO and NO_2 on the ZnO (2110) surface: a DFT study. Suf Sci. 2009;603:3389–99.
6. Chen M, Wang ZH, Han DM, Gu FB, Guo GS. High-sensitivity NO_2 gas sensors based on flower-like and tube-like ZnO nanomaterials. Sensor Actuat B-Chem. 2011;157:565–74.
7. Wang JX, Sun XW, Yang Y, Wu CML. N-P transition sensing behaviors of ZnO nanotubes exposed to NO_2 gas. Nanotechnology. 2009;20:4.
8. Barazzouk S, Tandon RP, Hotchandani S. MoO_3-based sensor for NO, NO_2 and CH_4 detection. Sensor Actuat B-Chem. 2006;119:691–4.
9. Wang XP, Yu SS, Yang HL, Zhang SX. Selective catalytic reduction of NO by C_2H_2 over MoO_3/HZSM-5. Appl Catal B- Environ. 2007;71:246–53.
10. Zhang DH, Liu ZQ, Li C, Tang T, Liu XL, Han S, et al. Detection of NO_2 down to ppb levels using individual and multiple In_2O_3 nanowire devices. Nano Lett. 2004;4:1919–24.
11. Prades JD, Cirera A, Morante JR. First-principles study of NO_x and SO_2 adsorption onto SnO_2(110). J Electrochem Soc. 2007;154:H675–80.
12. Hyodo T, Sasahara K, Shimizu Y, Egashira M. Preparation of macroporous SnO_2 films using PMMA microspheres and their sensing properties to NO_x and H_2. Sensor Actuat B-Chem. 2005;106:580–90.
13. Wu QP, Yang CC, van de Krol R. A dopant-mediated recombination mechanism in Fe-doped TiO_2 nanoparticles for the photocatalytic decomposition of nitric oxide. Catal Today. 2014;225:96–101.
14. Oison V, Saadi L, Lambert-Mauriat C, Hayn R. Mechanism of CO and O_3 sensing on WO3 surfaces: first principle study. Sensor Actuat B-Chem. 2011;160:505–10.
15. Wang FG, Di Valentin C, Pacchioni G. DFT study of hydrogen adsorption on the monoclinic WO_3 (001) surface. J Phys Chem C. 2012;116:10672–9.
16. Santato C, Odziemkowski M, Ulmann M, Augustynski J. Crystallographically oriented mesoporous WO_3 films: synthesis, characterization, and applications. J Am Chem Soc. 2001;123:10639–49.
17. Li XL, Lou TJ, Sun XM, Li YD. Highly sensitive WO_3 hollow-sphere gas sensors. Inorg Chem. 2004;43:5442–9.
18. Baeck SH, Choi KS, Jaramillo TF, Stucky GD, McFarland EW. Enhancement of photocatalytic and electrochromic properties of electrochemically fabricated mesoporous WO_3 thin films. Adv Mater. 2003;15:1269–73.
19. Lee SH, Deshpande R, Parilla PA, Jones KM, To B, Mahan AH, et al. Crystalline WO_3 nanoparticles for highly improved electrochromic applications. Adv Mater. 2006;18:763–6.
20. Chen D, Ye JH. Hierarchical WO_3 hollow shells: dendrite, sphere, dumbbell, and their photocatalytic properties. Adv Funct Mater. 2008;18:1922–8.
21. Qin Y, Hua D, Liu M. First-principles study on NO_2-adsorbed tungsten oxide nanowires for sensing application. J Alloy Compd. 2014;587:227–33.
22. Cao BB, Chen JJ, Tang XJ, Zhou WL. Growth of monoclinic WO_3 nanowire array for highly sensitive NO_2 detection. J Mater Chem. 2009;19:2323–7.
23. Kaushik A, Khan R, Gupta V, Malhotra BD, Ahmad S, Singh SP. Hybrid cross-linked polyaniline-WO(3) nanocomposite thin film for NO(x) gas sensing. J Nanosci Nanotechno. 2009;9:1792–6.
24. Dutta A, Kaabbuathong N, Grilli ML, Di Bartolomeo E, Traversa E. Study of YSZ-based electrochemical sensors with WO_3 electrodes in NO_2 and CO environments. J Electrochem Soc. 2003;150:H33–7.
25. Balazsi C, Sedlackova K, Llobet E, Ionescu R. Novel hexagonal WO_3 nanopowder with metal decorated carbon nanotubes as NO_2 gas sensor. Sensor Actuat B-Chem. 2008;133:151–5.
26. Moon HG, Choi YR, Shim Y-S, Choi K-I, Lee J-H, Kim J-S, et al. Extremely sensitive and selective NO probe based on villi-like WO_3 nanostructures for application to exhaled breath analyzers. ACS Appl Mater Inter. 2013;5:10591–6.

27. Chen DL, Yin L, Ge LF, Fan BB, Zhang R, Sun J, et al. Low-temperature and highly selective NO-sensing performance of WO_3 nanoplates decorated with silver nanoparticles. Sensor Actuat B-Chem. 2013;185:445–55.
28. Li M, Altman EI, Posadas A, Ahn CH. The p(4 × 2) surface reconstruction on epitaxial WO_3 thin films. Suf Sci. 2003;542:22–32.
29. Kresse G, Hafner J. Ab initio molecular dynamics for open-shell transition metals. Phys Rev B. 1993;48:13115–8.
30. Kresse G, Furthmuller J. Efficient iterative schemes for ab initio total-energy calculations using a plane-wave basis set. Phys Rev B. 1996;54:11169–86.
31. Kresse G, Furthmuller J. Efficiency of ab-initio total energy calculations for metals and semiconductors using a plane-wave basis set. Comp Mater Sci. 1996;6:15–50.
32. Blochl PE. Projector augmented-wave method. Phys Rev B. 1994;50:17953–79.
33. Hammer B, Hansen LB, Norskov JK. Improved adsorption energetics within density-functional theory using revised Perdew-Burke-Ernzerhof functionals. Phys Rev B. 1999;59:7413–21.
34. Monkhorst HJ, Pack JD. Special points for Brillouin-zone integrations. Phys Rev B. 1976;13:5188–92.
35. Wanbayor R, Ruangpornvisuti V. A periodic DFT study on binding of Pd, Pt and Au on the anatase TiO_2 (001) surface and adsorption of CO on the TiO_2 surface-supported Pd. Pt and Au Appl Surf Sci. 2012;258:3298–301.
36. Dion M, Rydberg H, Schroder E, Langreth DC, Lundqvist BI. Van der Waals density functional for general geometries. Phys Rev Lett. 2004;92:4.
37. Tang W, Sanville E, Henkelman G. A grid-based Bader analysis algorithm without lattice bias. Appl Phy A-Mater. 2009;21:7.
38. Bader RFW. A Quantum Theory. New York: Oxford University Press; 1990.